ELSEVIER

Journal of Nuclear Materials 305 (2002) 124–133

journal of nuclear materials

www.elsevier.com/locate/jnucmat

Single-phase diffusion study in β-Zr(Al)

A. Laik, K. Bhanumurthy, G.B. Kale *

Materials Science Division, Bhabha Atomic Research Centre, Mumbai 400 085, India

Received 19 February 2002; accepted 9 July 2002

Abstract

The diffusion behaviour of Al and Zr was investigated in the β-Zr(Al) phase in the temperature range 1203–1323 K by employing single-phase diffusion couples of pure Zr/Zr–2.8 wt% Al. The interdiffusion coefficients show a small increase with increase in Al concentration and follow a quadratic compositional relation. The temperature dependence of the interdiffusion coefficients at various compositions was established. The activation energy for the interdiffusion coefficient decreases linearly with an increase in Al concentration. The intrinsic diffusivity of Zr is higher than that of Al in this phase field. The impurity diffusion coefficient of Al in β-Zr was determined by extrapolation of interdiffusion coefficients to limiting concentration of Al and it shows temperature dependence: $D_{\mathrm{Al}}^{\beta\text{-Zr}}(c_{\mathrm{Al}}=0)=5.567^{+2.65}_{-1.80}\times 10^{-6}\exp[(-220.08\pm 3.33)\ \mathrm{kJ}/RT]\ \mathrm{m}^2/\mathrm{s}$. A correlation between the impurity diffusion coefficients of various impurities in β-Zr and the atomic radii of the impurity atoms has been established and can be presented by the relation: $\log D_{\mathrm{imp}}^{\beta\text{-Zr}}\ (\mathrm{m}^2/\mathrm{s})=-14.57\pm 1.22+\exp[(4.84\pm 2.83)-(30.22\pm 2.66)r\ (\mathrm{nm})]$.

1. Introduction

Alloys based on Zr_3Al intermetallics are considered as potential structural materials for thermal nuclear reactors due to their low thermal neutron absorption cross-section, high melting point and high strength [1,2]. In the binary system of Zr–Al, two peritectiod reactions occur in a temperature interval of 100 K, i.e. between 1200 and 1300 K, which involve Zr_3Al. These two reactions, viz. $\beta\text{-Zr}+Zr_2Al\Longleftrightarrow Zr_3Al$ and $\beta\text{-Zr}+Zr_3Al\Longleftrightarrow \alpha Zr$ are important as they describe the formation and decomposition of the intermetallic compound Zr_3Al respectively. These reactions being peritectiod in nature, their kinetics are essentially controlled by diffusion processes. The only available data in the literature are on chemical diffusion coefficients in β-Zr(Al) and some intermetallic compounds of the Zr–Al system [3]. The data reported in [3] were determined using multiphase diffusion couples.

It is worth noting that Sprengel et al. [4] showed that the interdiffusion coefficients obtained from diffusion couple consisting of multiple phases differ from those consisting a single-phase. Kim and Chang [5] have reported results from a single-phase diffusion study in the NiAl phase. They showed a large difference in the activation energy for interdiffusion determined by multi-phase diffusion couples and single-phase diffusion couples. The large difference in the activation energy could be due to the fact that phase boundaries formed in multi-phase diffusion couples influence the diffusion flux to a large extent. The phase boundaries act as a source and sink for point defects, and the grain boundaries in an intermediate phase, formed in the process of annealing, can alter the overall diffusion rate in the system. Therefore the diffusion coefficients calculated from such experiments are not truly representative. Besides, no data for tracer diffusivity of aluminium (D_{Al}^{*}) in β-Zr exist in the literature. This is mainly due to the non-availability of a suitable radioactive isotope of Al that can be used as a tracer. The only isotope suited for such experiments is ^{26}Al, which has very low activity.

* Corresponding author.
E-mail address: gbkale@apsara.barc.ernet.in (G.B. Kale).

0022-3115/02/$ - see front matter
PII: S0022-3115(02)01028-0

The present work reports a detailed study of the diffusion behaviour of Al and Zr in the β-Zr(Al) phase field in the temperature range 1203–1323 K employing single-phase diffusion couples. The interdiffusion coefficients and their composition and temperature dependence have been established. The intrinsic diffusivities D_{Al} and D_{Zr} have been calculated from the marker movement by applying Darken's relations [6]. The impurity diffusion coefficient of Al in β-Zr and its temperature dependence are also determined by extrapolating the interdiffusivity values calculated by Hall's method, to the infinite dilution of the solute (Al). Tracer diffusivity values for Zr and Al in the β-Zr(Al) phase region are also calculated from the intrinsic diffusivity and the thermodynamic factor Φ using the Darken–Dehlinger relation [7].

2. Experimental procedure

2.1. Diffusion couple preparation

A Dilute alloy of Al in Zr with nominal composition Zr–2.8 wt% Al was prepared by arc melting proportionate mixture of pure (99.9%) Zr and pure (99.95%) Al under high purity argon atmosphere. The alloy was remelted several times to attain chemical homogeneity throughout the button. The composition of the alloy was determined by electron probe micro analysis (EPMA) and was confirmed to be having homogenous composition of Zr–2.8 wt% Al. The as cast button of the alloy was coated with fine alumina powder suspension in ethyl alcohol and encapsulated in a steel tube while maintaining a vacuum (10^{-1} Pa) inside. The steel jacketed alloy was subsequently hot rolled at 1233 K slowly with small amount of deformation in each pass, finally leading to 22% of overall deformation. The alumina coating was an essential step to avoid diffusion of Fe into the alloy from steel and the steel jacketing was to prevent oxygen from entering the system during the process of hot rolling. Samples of size $10 \times 8 \times 3$ mm^3 were cut from the rolled alloy. Similarly samples of pure Zr were also cut of nearly the same size. These samples were encapsulated in quartz tubes in He atmosphere and a pressure of about 16 kPa was maintained inside. The sealed samples were then annealed at 1250 K for 72 h. Annealing was done also to form stable coarse grain structure, which reduces the contribution of grain boundary diffusion in the diffusion annealing stage. EPMA on the alloy after annealing confirmed the composition to be Zr–2.8 wt% Al, indicating that there was no pick up of oxygen or Fe either in the rolling stage or in the subsequent annealing stages. The 10×8 mm^2 surfaces of the samples were prepared by grinding on successive grades of emery paper and then polishing on a lapping wheel with 0.25 μm diamond paste. The diffusion couples were made by keeping the polished surfaces of the pure Zr and the Zr–2.8 wt% Al pieces in contact with each other under a pressure of about 5 MPa in an Inconel die and then heating in vacuum better than 10^{-3} Pa at 1173 K for 1 h. Tungsten wires of 6–8 μm diameter were used as markers between the two pieces of the couple. EPMA across the interface of the as bonded couples showed a diffusion width typically in the range of 5–8 μm which is negligible compared to diffusion width of around 200 μm observed in the annealed couples. The couples were then sealed in quartz capsules in He atmosphere and diffusion annealed in a preheated resistance heating furnace in the temperature range 1203–1323 K for 72 h. The temperature of the furnace was controlled within ±1 K by a proportional temperature controller. After the isochronal heat treatment, the capsules were quenched in water.

2.2. Metallographical preperation

The diffusion annealed couples were sectioned perpendicular to the bond interface using a slow-speed diamond saw. These samples were mounted, ground on various grades of emery papers and then polished on a lapping wheel with 0.25 μm diamond paste.

2.3. Electron microprobe analysis

The polished, unetched diffusion couples were analysed using a Cameca SX100 electron probe micro analyser equipped with three wavelength dispersive spectrometers. The operating voltage and beam current were kept at 20 kV and 20 nA respectively. Pure Zr and pure Al were used as standards for the analysis. Pentaerythritol and thallium acid pthalate (TAP) crystals were used for diffraction of Zr–Lα and Al–Kα lines respectively. The standard PAP correction program was used for atomic number (Z), absorption (A) and fluorescence (F) corrections. Quantitative analysis on point-to-point basis was done at a regular interval of 1–2 μm by scanning the sample across the bonding interface to determine the concentration profile. For each sample, at least three scans were taken at different locations to confirm the consistency of the concentration profiles.

3. Data analysis

The most widely used method to determine the concentration dependent interdiffusion coefficient is the Boltzmann–Matano method [8,9]. But as the method involves numerical solution of the Fick's second law and estimation of slope of the concentration profile at the point concerned, the major drawback of the method is that it incorporates a lot of error in calculation of the slope at the extreme ends of the profile. Since Hall's

method is analytical, one can yield sufficiently accurate diffusion data in such a low concentration range [10]. Therefore to eliminate such erroneous results, Hall's analytical method [10,11] was used instead for the composition range $0 \leqslant C_{Al} \leqslant 2$ at.%, and Boltzmann–Matano method for $C_{Al} \geqslant 2$ at.%.

In a binary system A–B, the interdiffusion coefficient at composition C^* is calculated by the relation

$$\widetilde{D}_{AB}(C^*) = -\frac{1}{2t}\left(\frac{dx}{dC}\right)_{C=C^*}\int_{C=C^{-\infty}}^{C^*}(x-x_0)\,dC \tag{1}$$

with the initial boundary condition as: at $t=0$ and $x \leqslant x_0$, $C = C^{-\infty}$ and at $t=0$ and $x \leqslant x_0$, $C = C^{+\infty}$, where t is the time of annealing, $(dx/dC)_{C=C^*}$ is the inverse of the concentration gradient at C^*, $C^{-\infty}$ is the concentration at the extreme left end, $C^{+\infty}$ is the concentration at the right end and x_0 is the position of the Matano interface (MI).

In Hall's method, a variable λ is defined in such a way that,

$$\frac{C^*}{C_0} = \frac{1}{2}(1+\mathrm{erf}(\lambda)), \tag{2}$$

where C^* is the solute concentration at time t and position x with respect to the MI, $C_0 = |C^{+\infty} - C^{-\infty}|$ and $\mathrm{erf}(\lambda)$ is the error function of λ. λ is found to bear a linear relationship with the variable $\eta(= x/\sqrt{t})$, as

$$\lambda = h\eta + k. \tag{3}$$

The concentration dependent interdiffusion coefficient $\widetilde{D}(C)$ can be determined from the values of h and k by the following relation [10]:

$$\widetilde{D}(C^*) = \frac{1}{4h^2} + \frac{k\sqrt{\pi}}{4h^2}(1+\mathrm{erf}(\lambda))\exp(\lambda^2). \tag{4}$$

The intrinsic diffusivities of the constituent elements A and B, i.e. D_A and D_B, at the marker positions were calculated by using Darken's equation [6,12] and the velocity of the markers, v

$$\widetilde{D}_{AB} = (D_A N_B + D_B N_A), \tag{5a}$$

$$v = \frac{\Delta x}{2t} = (D_A - D_B)\left(\frac{dC}{dx}\right), \tag{5b}$$

where Δx is the displacement of the markers from the original interface in the annealing time t, and (dC/dx) is the concentration gradient at the marker location.

The tracer diffusivities were calculated from the intrinsic diffusivities by the Darken–Dehlinger relation [7]

$$D^* = D/\Phi, \tag{6}$$

where, Φ is the thermodynamic factor. The method of calculation of Φ is described in Appendix A.

4. Results and discussions

4.1. Microstructure

The optical micrograph in Fig. 1 shows the microstructure of the Zr–2.8 wt% Al alloy used for making diffusion couples. It is evident from the microstructure that the prior β-phase had a coarse-grained structure. The nearly straight grain boundaries indicate that the grains are equiaxed and strain free. The average size of the prior β grains is around 200 μm.

Fig. 2 shows a backscattered electron image at the interface of a diffusion couple annealed at 1203 K. The tungsten marker can be seen very prominently. All the couples show excellent bonding at the interface, with practically no cracks, pores or voids present in the diffusion zone.

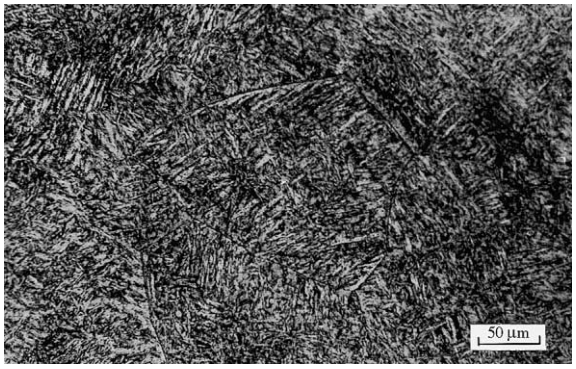

Fig. 1. Optical micrograph of Zr–2.8 wt% Al alloy used for making couple with pure Zr.

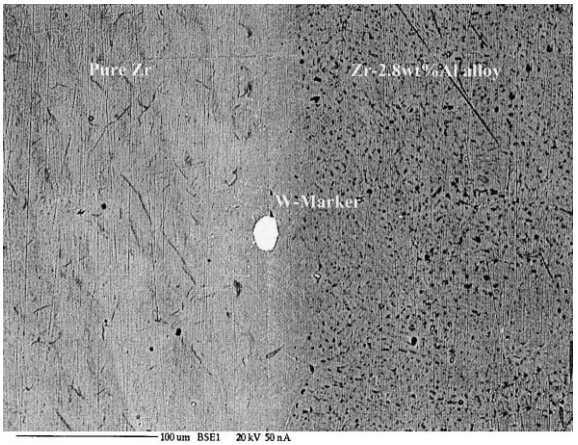

Fig. 2. Backscattered electron image of the interface of Zr/Zr–2.8 wt% Al couple annealed at 1203 K for 72 h.

4.2. Interdiffusion in the β-Zr(Al) phase

A typical concentration profile across the diffusion zone, obtained after annealing a diffusion couple for 72 h at 1293 K, is shown in Fig. 3. This is a typical solid solution type of concentration-distance curves across the interface of the couples. The concentration profile is asymmetric with respect to the MI. Aluminium diffuses deeper into pure zirconium as compared to the extent zirconium diffuses into the Zr–2.8 wt% Al alloy. This asymmetry is attributed to the wide difference in the intrinsic diffusivities of the two elements as discussed in Section 4.3. During the process of annealing, the initial compositions of the individual pieces of the couples are preserved at the ends, thereby fulfilling the requirement of the infinite geometry. Hence, the interdiffusion coefficient could be calculated by Boltzmann–Matano method and Hall's method in the suitable concentration domains as already stated in Section 3. Fig. 4 shows a plot of λ versus η corresponding to Fig. 3. It is observed that in all the temperatures investigated, these plots are nearly linear in the composition range of the present study. The values of slope h and intercept k (of Eq. (3)) are determined at each temperature by a least square fit through the data points. These values are used in Eq. (4) to calculate the analytical value of the interdiffusion coefficient $\widetilde{D}$ by Hall's method in the concentration range $0 \leqslant C_{Al} \leqslant 2$ at.%. For the rest of the concentration range, i.e. $C_{Al} \geqslant 2$ at.%, Boltzmann–Matano method (Eq. (1)) was used to calculate the interdiffusion coefficient $\widetilde{D}$. For a diffusion coefficient calculation by the Botlzmann–Matano method, the concentration profiles were fit with a curve using the cubic spline method, and the flux was determined by numerical integration of the area under the curve, and the slope was calculated by

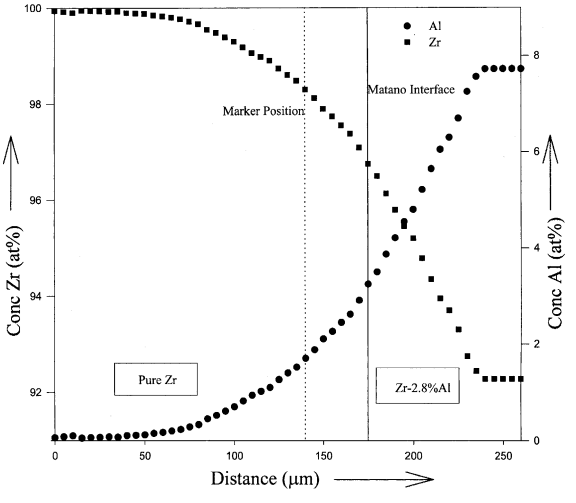

Fig. 3. Concentration profile of Zr/Zr–2.8 wt% Al couple annealed at 1293 K for 72 h.

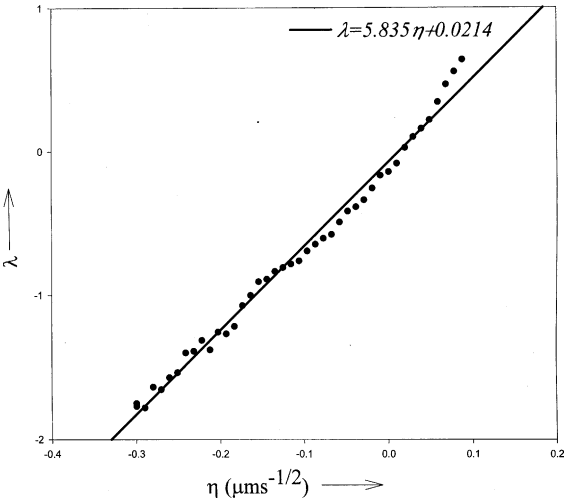

Fig. 4. Variation of λ and η in sample annealed at 1293 K for 72 h.

numerical differentiation of the profile. Table 1 shows the interdiffusion coefficient values at various conditions of temperature and composition. The interdiffusion coefficients in the present study are about an order of magnitude higher than those reported by Gukelberger and Steeb [3]. This may be due to the influence of the interfaces in the multi-phase diffusion couples used by them.

4.2.1. Concentration dependence of interdiffusion coefficient

The concentration dependence of the interdiffusion coefficients at various temperatures of study is presented in Fig. 5. It is evident from the figure that in the whole temperature range the interdiffusion coefficient $\widetilde{D}$ increases with increasing concentration of Al. But the increase in $\widetilde{D}$ with concentration is higher at higher concentration of Al than that at lower concentration of Al. The interdiffusion coefficients at various temperatures are fitted in a quadratic relation of the type $\widetilde{D} = P + QC_{Al} + RC_{Al}^2$. The values of the parameters P, Q and R for various temperatures are given in Table 2. Gukelberger and Steeb [3] have reported interdiffusion coefficients $\widetilde{D}$ in the β-Zr(Al) phase, determined from multi-phase diffusion couple experiments in the temperature range 1273–1573 K. They also showed an increase in the interdiffusion coefficient with an increase in Al concentration.

Ti and Zr, belonging to the group IVB of the periodic table, behave similarly as far as the diffusion processes are concerned [13]. Therefore, the interdiffusion behaviour of the Zr–Al system is worth comparing with that of the Ti–Al system. Hirano and Iijima [14] reported interdiffusion studies employing both single-phase and multi-phase diffusion couples in the temperature range

Table 1
Values of the interdiffusion coefficients at various temperature and comositions

Composition (at.%)	Interdiffusion coefficient (10^{15} m^2/s)				
	1203 K	1233 K	1263 K	1293 K	1323 K
1	1.76	2.41	4.23	7.78	11.37
2	1.86	2.45	4.28	7.83	11.42
4	2.09	2.54	4.40	7.93	11.57
6	2.50	2.74	4.80	8.26	12.49

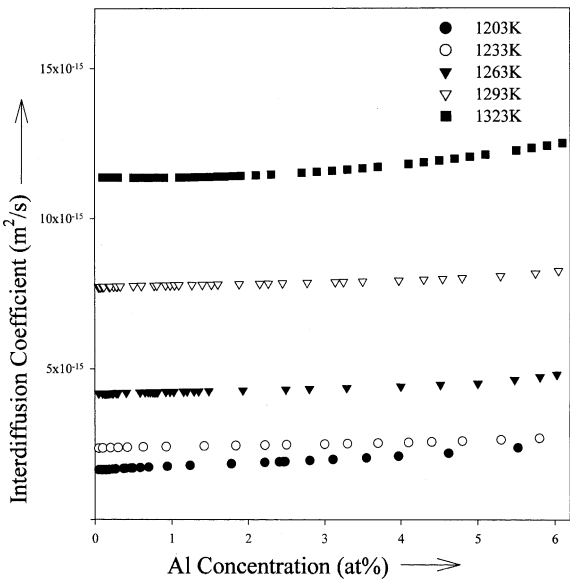

Fig. 5. Concentration dependence of interdiffusion coefficient.

973–1523 K. They showed a similar increase in $\widetilde{D}$ in the β-Ti(Al) with an increase in Al concentration. Addition of Al to Zr decreases the solidus temperature line in the Zr–Al phase diagram [15]. The activation energy of diffusion is directly related to the solidus temperature [16]. Therefore with increase in Al concentration solidus temperature and hence activation energy decreases and the diffusivity increases.

Table 2
Values of the parameters P, Q and R in the relation $\widetilde{D} = P + QC_{Al} + RC_{Al}^2$ for the composition dependence of the interdiffusion coefficients

Temperature (K)	$P \times 10^{15}$ (m^2/s)	$Q \times 10^{18}$ (m^2/s at.%$^{-1}$)	$R \times 10^{18}$ (m^2/s at.%$^{-2}$)
1203	1.69	16.65	23.87
1233	2.33	3.95	11.17
1263	4.19	−3020.20	590.89
1293	7.71	20.77	9.20
1323	11.36	−15.14	38.43

4.2.2. Temperature dependence of interdiffusion coefficient

In order to establish the temperature dependence of the interdiffusion coefficient $\widetilde{D}$, $\ln\widetilde{D}$ is plotted against the reciprocal of absolute temperature of diffusion annealing for various compositions in Fig. 6. A linear relationship in this plot shows that $\widetilde{D}$ follows an Arrhenius type of relationship, $\widetilde{D} = \widetilde{D}_0 \exp(-Q/RT)$. $\widetilde{D}_0$ is the pre-exponential factor, Q is the activation energy and T is the absolute temperature. The values of Q and $\widetilde{D}_0$ for various compositions were calculated by the least square method and are shown in Table 3. The activation energy for interdiffusion, varies from 215.8 to 189.9 kJ/mol in the concentration range 2 at.% $\leqslant C_{Al} \leqslant$ 6 at.%. The $\widetilde{D}_0$ and Q values in the present study are comparable to those reported in Ref. [3] for $C_{Al} \geqslant 8$ at.%. The activation energy for interdiffusion, Q, in β-Zr(Al) decreases

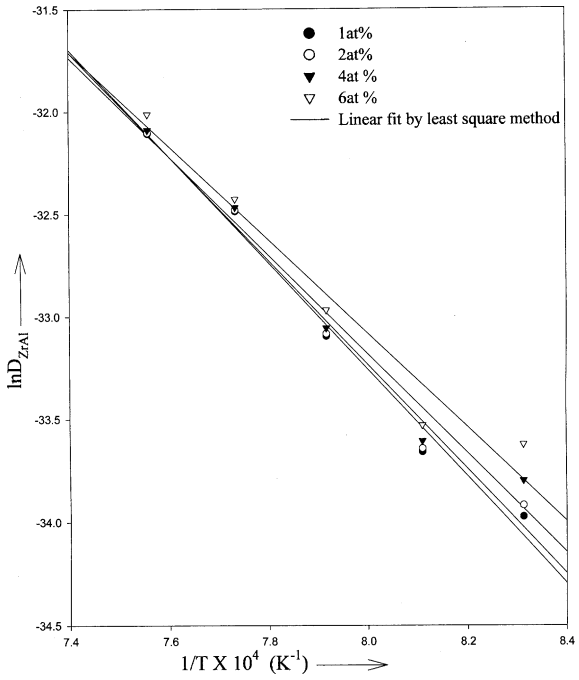

Fig. 6. Temperature dependence of interdiffusion coefficient at various compositions of Al.

Table 3
Pre-exponential factor and activation energy for interdiffusion at various compositions of Zr and Al

Composition Al (at.%)	Pre-exponential factor ($D_0 \times 10^6$) (m^2/s)	Activation energy Q ($kJ\,mol^{-1}$)
1[a]	$3.76^{+1.77}_{-1.21}$	215.8 ± 3.3
2[a]	$2.02^{+1.08}_{-0.75}$	209.1 ± 3.2
4[a]	$5.34^{+0.38}_{-0.27}$	194.9 ± 3.1
6[a]	$0.37^{+0.14}_{-0.10}$	189.9 ± 2.9
8[b]	0.92	179
10[b]	2.3	169

[a] Present study.
[b] Ref. [3].

linearly with an increase in concentration of Al, as shown in Fig. 7, and follows a relation

$$Q\ (\mathrm{kJ/mol}) = 219.9 - 5.36 C_{\mathrm{Al}}\ (\mathrm{at.\%}).$$

4.3. Marker movement, intrinsic diffusion and tracer diffusion

4.3.1. Intrinsic diffusion coefficients

It was observed that the tungsten wires used as markers in the experiments, move towards the pure zirconium side on annealing as seen from Fig. 3. This is due to the Kirkendall effect and suggests that the intrinsic diffusion coefficient of Zr is higher than Al, $D_{\mathrm{Zr}} > D_{\mathrm{Al}}$. The extent of displacement of the markers from their original positions depends upon the time and the temperature of annealing. It is assumed that this displacement is controlled purely by diffusional processes and hence the displacement Δx, is proportional to the square root of the time of annealing t, i.e. $\Delta x \propto \sqrt{t}$.

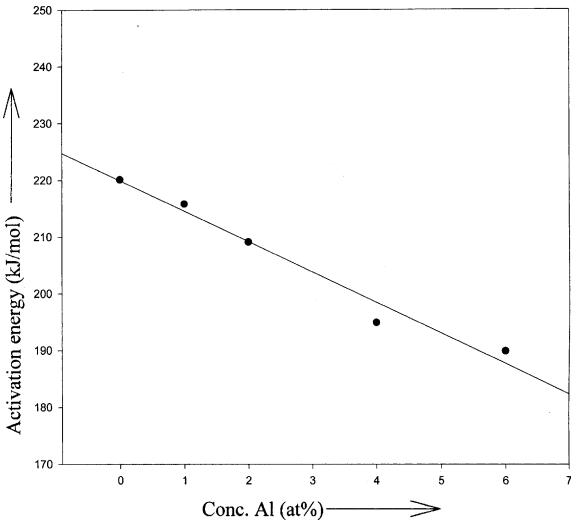

Fig. 7. Composition dependence of activation energy for interdiffusion coefficient.

The intrinsic diffusion coefficients of Zr (D_{Zr}) and of Al (D_{Al}), at the concentration of the marker plane, were calculated by Darken's relationships [6,12] given in Eqs. (5a) and (5b). Here the velocity of the markers, $v = \Delta x/2t$, was taken as the average velocity over the whole time period of annealing, t. It was found that the marker plane has an average composition of 2 at.% Al. The values of the intrinsic diffusion coefficients D_{Zr} and D_{Al} are given in Table 4. It is seen from the table that D_{Zr} is larger than D_{Al} in the whole temperature range.

It is also noteworthy here that the values of D_{Zr} and D_{Al} are within one order of magnitude. This indicates that vacancy exchange mechanism is operative in the present case [17]. The solute (Al) and solvent (Zr) atoms share the same sites and exchange with the same vacancies.

Following the Lazarus' valence theory for impurity diffusion [18], lower valent impurity diffuses slower in the higher valent matrix. Zr is tetravalent and Al is trivalent. This explains the slower diffusivity of Al in Zr.

4.3.2. Tracer diffusion coefficients

The tracer diffusion coefficients, D^*_{Zr} and D^*_{Al}, corresponding to the intrinsic diffusivities of zirconium and aluminium respectively, were calculated by Darken–Dehlinger relation [7] as shown in Eq. (6). The thermodynamic factor Φ for Zr–Al system is calculated for all the temperatures of investigation. Details are given in Appendix A. It is shown that in the concentration range $0 \leqslant C_{\mathrm{Al}} \leqslant 8$ at.% the value of Φ is independent of the composition. The values of the self-diffusivities D^*_{Zr} and D^*_{Al} and the intrinsic diffusivities D_{Zr} and D_{Al} of Zr and Al are tabulated in Table 4 with respect to the temperature of annealing.

4.4. Impurity diffusion of Al in β-Zr

According to the Darken's relation [6], the interdiffusion coefficient in an infinitely dilute solid solution corresponds to the impurity diffusion coefficient of the solute in the solvent matrix. The impurity diffusion coefficient of Al in β-Zr is determined by extrapolating the $\widetilde{D}$ values in the range $0 \leqslant C_{\mathrm{Al}} \leqslant 2$ at.%, calculated by Hall's method, to $C_{\mathrm{Al}} \to 0$. In the narrow composition range $0 \leqslant C_{\mathrm{Al}} \leqslant 2$ at.%, $\widetilde{D}$ bears a linear relationship with C_{Al} of the type $\widetilde{D} = a + bC_{\mathrm{Al}}$. The impurity diffusion coefficient of Al in β-Zr is evaluated by extrapolating $\widetilde{D}$ to $C_{\mathrm{Al}} \to 0$. Here we shall denote impurity diffusion of Al in β-Zr as $D^{\beta\text{-Zr}}_{\mathrm{Al}}(C_{\mathrm{Al}} = 0)$. Table 5 shows the values of $D^{\beta\text{-Zr}}_{\mathrm{Al}}(C_{\mathrm{Al}} = 0)$ at various temperatures of investigation. The logarithm of $D^{\beta\text{-Zr}}_{\mathrm{Al}}(C_{\mathrm{Al}} = 0)$ is plotted against the inverse of absolute temperature in Fig. 8. The frequency factor D_0 and the activation energy Q have been estimated by fitting a straight line (solid line in Fig. 8) to the

Table 4
Intrinsic and self diffusion coefficients at the marker positions at various temperatures

Temperature (K)	$D_{Al} \times 10^{15}$ (m^2/s)	$D_{Zr} \times 10^{15}$ (m^2/s)	$D^*_{Al} \times 10^{15}$ (m^2/s)	$D^*_{Zr} \times 10^{15}$ (m^2/s)
1203	1.67	3.45	1.40	2.90
1233	2.39	4.74	2.01	3.99
1263	4.16	6.88	3.51	5.81
1293	7.75	11.03	6.56	9.34
1323	11.35	14.92	9.64	12.67

Table 5
Impurity diffusion coefficient of Al in β-Zr

Temperature (K)	Impurity diffusivity $D^{\beta\text{-Zr}}_{Al}(c_{Al} = 0) \times 10^{15}$ (m^2/s)
1203	1.69
1233	2.33
1263	4.19
1293	7.71
1323	11.36

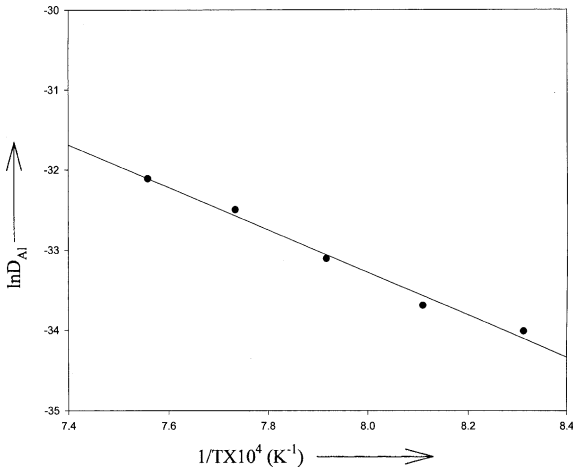

Fig. 8. Temperature dependence of impurity diffusivity of Al in β-Zr.

points by the least square method. The temperature dependence can be expressed by an Arrhenius relation:

$$D^{\beta\text{-Zr}}_{Al}(c_{Al} = 0) = 5.567^{+2.65}_{-1.80} \times 10^{-6} \exp[(-220.08 \pm 3.33)\ \text{kJ}/RT]\ \text{m}^2/\text{s}. \quad (7)$$

The activation energy of self-diffusion of Zr in β-Zr is 115.78 kJ/mol [19] as compared to 220.08 kJ/mol for the impurity diffusion of Zr in β-Zr. The difference between the activation energy values, ΔQ ($Q^{Al} - Q^{self}$) is 104.3 kJ/mol. Such a positive value suggests a rather low impurity-vacancy binding energy according to the theory of vacancy diffusion [20,21]. Due to low impurity-vacancy binding energy, solvent-vacancy exchange is more dominant. This explains the higher diffusivity of the solvent (Zr) than solute (Al).

4.4.1. Interrelation between impurity diffusion parameters

The diffusion parameters of impurity diffusion of Al in β-Zr, i.e. activation energy Q^{Al} and the pre-exponential factor D_0^{Al}, are compared with that of its counterparts in other β-Zr–X systems (X = Co, Mn, Sn, V, Be, Fe, Ag and Ta) [19]. Both the values were found to be on the higher side. Several empirical correlations between the pre-exponential factor D_0 and the activation energy Q for impurity diffusion in metals are available in the literature [22–24]. Lazarus [18] derived expressions for D_0^{imp} and Q^{imp}, which includes parameters whose values depend upon the difference in ionic charge between solvent and solute ions. When transition metals are involved, as in the present case, there are uncertainties in attributing proper valance to them. Swalin [24] derived an equation based on the Lazarus theory to correlate the frequency factor, D_0, and the activation energy, Q, in which the charge of the impurity atom and the solvent is not involved. According to Swalin [24] a quantity ($\mathrm{d}\log D_0/\mathrm{d}Q$) should remain constant for different impurity elements in a particular solvent. The values of $\log D_0$ and Q for impurity diffusion of various elements in β-Zr are plotted in Fig. 9. Data for Al impurity diffusion matches close to the straight line of least square fit. The value of the slope of the straight line 4.52×10^{-3} mol/J, is comparable with the values of the impurity diffusion in other metals e.g. Ni ($(2.67 \pm 0.2) \times 10^{-2}$) [25] and Ag and Cu [26]. Later on Beke et al. [23] proposed a general expression for impurity diffusion. They showed that in a plot of $\ln(D_0^{imp}/D_0^{self})$ versus $\Delta Q/T_m$, the data points for various impurity elements should fall in a straight line. Such a plot for impurity diffusion in β-Zr is shown in Fig. 10. A straight line is drawn by the least square method and has a slope of 1.0126×10^{-2} mol K/J. The value of the slope is in excellent agreement with similar values reported earlier [23] for Al ($(9.3 \pm 0.7) \times 10^{-2}$ mol/J K), Ag ($(6.7 \pm 0.4) \times 10^{-2}$ mol/J K) and Cu ($(4.3 \pm 0.9) \times 10^{-2}$ mol/J K). All the elements, including Al, lie close to the straight line, and therefore a good agreement is obtained between the values of various elements. The impurity diffusion coefficient value of Al, therefore, is consistent

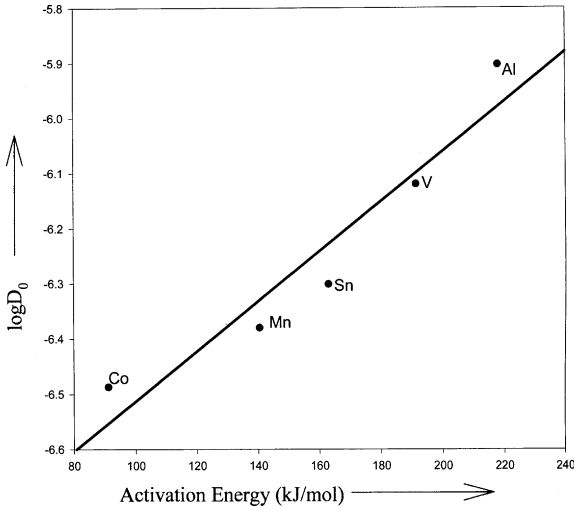

Fig. 9. Variation of pre-exponential factor with activation energy for various impurity atoms in β-Zr.

with the related theories of Swalin [24] (a refined form of Lazarus' theory) and Beke [23].

4.4.2. Atom size effect on impurity diffusion

Extensive work has been reported to correlate the impurity diffusion coefficient of different elements in metal solvents with the size of the impurity atoms [27–29]. Hood [30] showed that a close correlation exists between impurity diffusivity and the atomic size. The two can be related by an expression of the type

$$\log D = A + \exp(B - Cr), \tag{8}$$

where A, B and C are constants for the host metal and r is the atomic radius of the impurity atom. Such expressions were derived for Pb, α-Zr and Cu [30]. Fig. 11 shows a plot of log D for impurity diffusivities of various elements in β-Zr against r, their atomic radii. The data points are fitted to an expression of the type Eq. (7) by a least square curve fitting method. This fit produced a relation

$$\log D_{\text{imp}}^{\beta\text{-Zr}}\left(\frac{\text{m}^2}{\text{s}}\right) = -14.57 \pm 1.22 + \exp[(4.84 \pm 2.83) - (30.22 \pm 2.66)r\ (\text{nm})].$$

Al was found to be placed very close to the curve. This shows good correlation between the impurity diffusivity of Al with that of other elements in β-Zr.

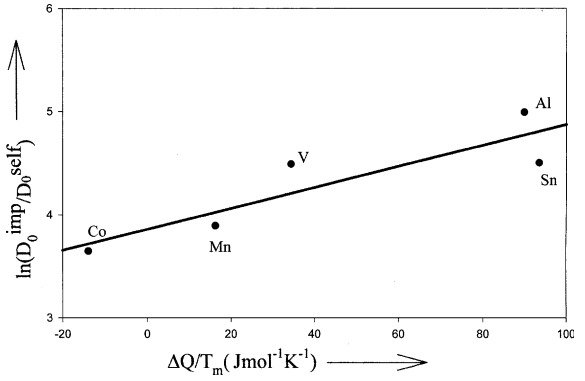

Fig. 10. Variation of $\ln(D_0^{\text{imp}}/D_0^{\text{self}})$ with $\Delta Q/T_{\text{m}}$ for various impurity atoms in β-Zr.

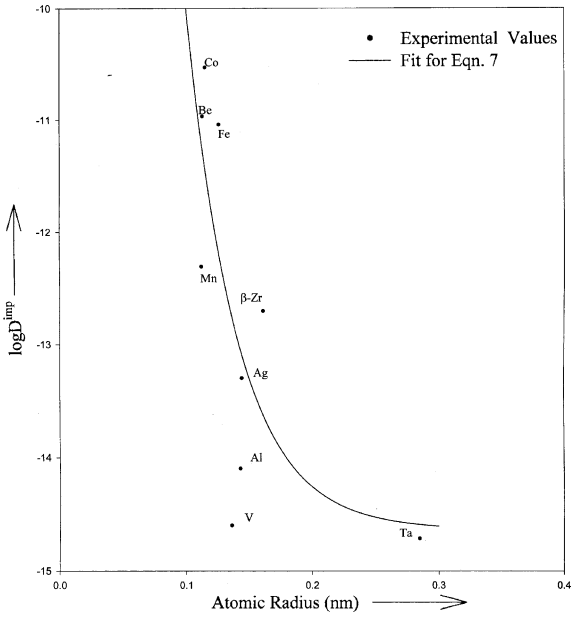

Fig. 11. Variation of impurity diffusivity in β-Zr with the atomic size.

5. Conclusions

From the single-phase diffusion couple experiments, it was found that the interdiffusion coefficient $\widetilde{D}$ continuously increases with concentration of Al in the range $C_{\text{Al}} < 6$ at.% Al and follows a quadratic type $\widetilde{D} = P + QC_{\text{Al}} + RC_{\text{Al}}^2$ of relation. The interdiffusion coefficient $\widetilde{D}$ shows an Arrhenius type of temperature dependence in the range of 1203–1323 K. The activation energy value for interdiffusion varies from 215.8 to 189.9 kJ/mol. A linear decrease in the activation energy for interdiffusion was observed with increasing C_{Al} in the concentration range $C_{\text{Al}} < 6$ at.%. The intrinsic diffusion coefficient for Zr is higher than that of Al in the β-Zr(Al) phase, as shown by the marker movement. This can be explained by the positive difference in the activation energies ($Q^{\text{imp}} - Q^{\text{self}}$), which indicates very low impurity-vacancy binding energy. The main mechanism of

diffusion in the β-Zr(Al) phase field is through vacancy exchange. The temperature dependence of impurity diffusivity of Al in β-Zr is

$$D_{\mathrm{Al}}^{\beta\text{-Zr}}(c_{\mathrm{Al}}=0)=5.56^{+2.65}_{-1.80}\times 10^{-6}\exp[(-220.08\pm 3.33)\ \mathrm{kJ}/RT]\ \mathrm{m}^2/\mathrm{s}.$$

The impurity diffusivity values are found to be consistent with Swalin's and Beke's theories. A relation between impurity diffusivity in β-Zr and atomic radii can be represented by the equation

$$\log D_{\mathrm{imp}}^{\beta\text{-Zr}}\left(\frac{\mathrm{m}^2}{\mathrm{s}}\right)=-14.57\pm 1.22+\exp[(4.84\pm 2.83)-(30.22\pm 2.66)r\ (\mathrm{nm})].$$

The diffusivity value for Al is in conformation to this relation.

Acknowledgements

The authors are grateful to Dr P. Mukhopadhyay, Head, Physical Metallurgy Section, Dr P.K. De, Head, Materials Science Division and Dr S. Banerjee, Director, Materials Group, BARC for their keen interest in the work. The authors also thank Mr P.S. Gawde for his help in carrying out the experiments.

Appendix A. Calculation of thermodynamic factor

The free energy of mixing for an n component solid solution at the absolute temperature T is given by

$$\Delta F_{\mathrm{mix}}=RT\sum_{i=1}^{n}N_i\ln a_i, \tag{A.1}$$

where, N_i and a_i are mole fraction and activity, respectively, of component i. For an ideal solid solution, the activity of a component is equal to its mole fraction, and hence the above relation takes the form

$$\Delta F_{\mathrm{mix}}^{\mathrm{ideal}}=RT\sum_{i=1}^{n}N_i\ln N_i. \tag{A.2}$$

For a deviation from ideal behaviour, the extent of deviation is quantified usually by the excess free energy of mixing denoted by $\Delta F_{\mathrm{mix}}^{\mathrm{excess}}$, in such a way that $\Delta F_{\mathrm{mix}}=\Delta F_{\mathrm{mix}}^{\mathrm{ideal}}+\Delta F_{\mathrm{mix}}^{\mathrm{excess}}$. As $a_{\mathrm{i}}=\gamma_{\mathrm{i}}N_{\mathrm{i}}$, where γ_i is the activity coefficient of component i,

$$\Delta F_{\mathrm{mix}}^{\mathrm{excess}}=RT\sum_{i=1}^{n}N_i\ln\gamma_i. \tag{A.3}$$

For a binary system, $\Delta F_{\mathrm{mix}}^{\mathrm{excess}}=RT(N_1\gamma_1+N_2\gamma_2)$. The free energy of mixing for a binary system can be expressed mathematically by

$$\Delta F_{\mathrm{mix}}^{\mathrm{excess}}=N_1N_2\sum_{j=0}^{m}(a_j+a'_jT)(N_1-N_2)^j. \tag{A.4}$$

For a regular solution $m=0$, for a sub-regular solution, $m=1$ and for a real solution the value of $m>1$ but generally does not exceed 2 [31]. In our calculation we consider $m=2$ assuming real solution. The parameters a_j and a'_j for BCC solid solution phase in the Zr–Al system, used in the present calculations are taken from the literature [32] and are shown in Table 6.

As in the present study we are concerned with dilute alloys, the activity of solvent Zr is nearly equal to its mole fraction and we assume $\gamma_{\mathrm{Zr}}=1$. Hence Eq. (A.3) becomes, $\Delta F_{\mathrm{mix}}^{\mathrm{excess}}=RTN_{\mathrm{Al}}\ln\gamma_{\mathrm{Al}}$. Combining this with Eq. (A.4) we get

$$\ln\gamma_{\mathrm{Al}}=\frac{N_{\mathrm{Zr}}}{RT}\sum_{j=0}^{2}(a_j+a'_jT)(N_1-N_2)^j. \tag{A.5}$$

The values of γ_{Al} were calculated at various temperatures and compositions using Eq. (A.5) and then subsequently the values of activity a_{Al} were calculated using $a_{\mathrm{Al}}=N_{\mathrm{Al}}\gamma_{\mathrm{Al}}$. As a convention, the thermodynamic factor Φ, which also is a measure of the deviation from ideal behaviour, is expressed as

Table 6
Solid solution parameters, in BCC structure of Zr–Al system

Parameters	J mol^{-1}	Parameters	J mol^{-1}K^{-1}
a_0	−80850	a'_0	−25
a_1	−11000	a'_1	0
a_2	10000	a'_2	0

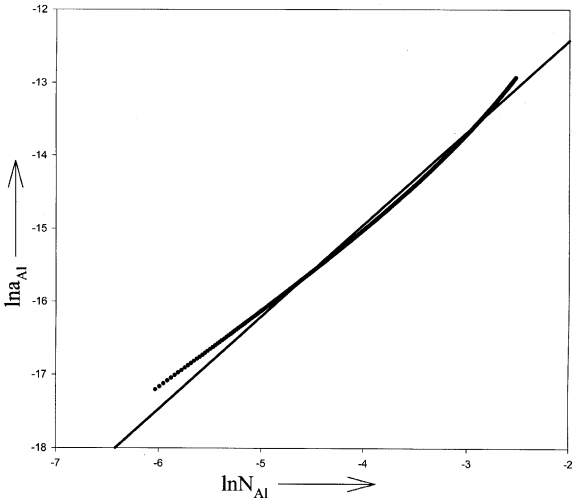

Fig. 12. Concentration dependence of activity of solute Al in β-Zr.

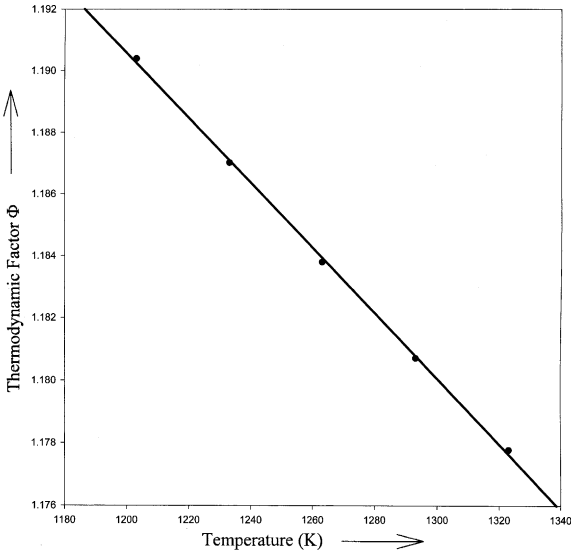

Fig. 13. Temperature dependence of thermodynamic factor Φ.

$$\Phi = 1 + \frac{\partial(\ln \gamma)}{\partial(\ln N)}$$

or

$$\Phi = \frac{\partial(\ln a)}{\partial(\ln N)}.$$

It is observed that in the plot of $\ln a_{\mathrm{Al}}$ versus $\ln N_{\mathrm{Al}}$ at 1203 K (shown in Fig. 12), the slope remains fairly constant in the concentration range of $0 \leqslant N_{\mathrm{Al}} \leqslant 0.08$. Hence the factor Φ is taken to be independent of concentration in this range. Therefore at a particular temperature the relation $\ln a_{\mathrm{Al}} = \lambda + \Phi \ln N_{\mathrm{Al}}$ holds. The values of Φ at different temperatures are calculated from the slope of the straight line fitted to the data points by the least square method in the $\ln a_{\mathrm{Al}}$ versus $\ln N_{\mathrm{Al}}$ plot. It is clear from Fig. 13 that the thermodynamic factor Φ bears a linear relationship with the absolute temperature T with a regression coefficient value of 0.999. The relation is

$$\Phi = 1.316 - 1.051 \times 10^{-4} T,$$

where T is absolute temperature.

References

[1] E.M. Schulson, in: J.H. Westbrook, R.L. Fleischer (Eds.), Intermetallic Compounds, vol. 2, John Wiley, 1994, p. 133.
[2] E.M. Schulson, J. Nucl. Mater. 57 (1975) 98.
[3] A. Gukelberger, S. Steeb, Z. Metallkd. 69 (1978) 255.
[4] W. Sprengel, N. Oikawa, H. Nakajima, Proceedings of the Workshop on Defects, Dynamics and Diffusion in Intermetallics, Vienna, Austria, 1994.
[5] S. Kim, Y.A. Chang, Metall. Mater. Trans. A 31A (2000) 1519.
[6] L.S. Darken, Trans. AIME 175 (1948) 184.
[7] J. Philibert, Atom movements: diffusion and mass transport in solids, Les Editions de Physique, Les Ulis, 1991, p. 204.
[8] C. Matano, Jpn. J. Phys. 8 (1933) 109.
[9] L. Boltzmann, Annal. Phys. 53 (1894) 960.
[10] L.D. Hall, J. Chem. Phys. 21 (1953) 87.
[11] J. Crank, Mathematics of Diffusion, Oxford University, Oxford, 1956, p. 219.
[12] P.G. Shewmon, Diffusion in Solids, 2nd Edn., The Minerals, Metals and Materials Society, Pennsylvania, PA, 1989, p. 135.
[13] J. Philibert, Atom movements: diffusion and mass transport in solids, Les Editions de Physique, Les Ulis, 1991, p. 119.
[14] K. Hirano, Y. Iijima, in: M.A. Dayananda, G.E. Murch (Eds.), Conference Proceedings of TMS-AIME Fall Meeting, Detroit, MI, 7 September 1984, 141.
[15] A. Peruzzi, J.P. Abraita, in: T.B. Massalski (Ed.), Alloy Binary Alloy Phase Diagrams, 2nd Ed., ASM International, Metals Park, OH, 1990, p. 241.
[16] A. Vignes, C.E. Birchenall, Acta Metall. 16 (1968) 1117.
[17] P.G. Shewmon, Diffusion in Solids, 2nd Ed., The Minerals, Metals and Materials Society, Pennsylvania, PA, 1989, p. 204.
[18] D. Lazarus, Phys. Rev. 93 (1954) 973.
[19] E.A. Brandes (Ed.), Smithels Metals Reference Book, 6th Ed., Butterworths, London, 1983.
[20] Le Claire, in: Physical Chemistry – An Advance Treatise: Solid State, vol. 10, Academic Press, London, 1970, p. 261.
[21] Le Claire, Philos. Mag. 7 (1962) 141.
[22] C. Zener, J. Appl. Phys. 22 (1951) 372.
[23] D. Beke, T. Geszti, G. Erdélyi, Z. Metallkd. 68 (1977) 444.
[24] R.A. Swalin, J. Appl. Phy. 27 (1956) 544.
[25] R.V. Patil, G.B. Kale, J. Nucl. Mater. 230 (1996) 57.
[26] J. Pelleg, Acta Metallurgica 14 (1966) 229.
[27] C.W. Owens, D. Turnbull, J. Appl. Phys. 43 (1972) 3933.
[28] W.K. Warburton, D. Turnbull, in: A.S. Nowick, J.J. Burton (Eds.), Diffusion in Solids: Recent Developments, Academic Press, New York, 1975, p. 171.
[29] G.M. Hood, R.J. Schultz, Acta Metall. 22 (1974) 459.
[30] G.M. Hood, J. Phys. F 8 (1978) 1677.
[31] N. Saunders, A.P. Miodowrick (Eds.), Calphad-Calculation of Phase Diagrams – A Comprehensive Guide, Pergamon, New York, 1998.
[32] N. Sunders, V.G. Rivlin, Mater. Sci. Tech 2 (1986) 521.